

Supplementary Material

October 3, 2025

1 Theoretical Model

A mechanical model of the flexible riser carcass layer under flat-plate compression is first established, as illustrated in Figure 1. Owing to the geometric symmetry of the carcass cross-section, only one-quarter of the structure is considered in the subsequent analysis to simplify the model. The structure is idealised as a curved beam spanning from point A to point B.

When a longitudinal compressive force F is applied to the plate, the internal force equilibrium at an arbitrary cross-section located at angle φ can be expressed as:

$$\begin{cases} N_\varphi = \frac{1}{2}F \cdot \sin \varphi \\ Q_\varphi = \frac{1}{2}F \cdot \cos \varphi \\ M_\varphi = M_A - \frac{1}{2}FR \cdot \sin \varphi \end{cases} \quad (1)$$

where N_φ , Q_φ , and M_φ are the axial force, shear force, and bending moment acting on the φ angle location, respectively.

The governing differential equation for the deflection curve of the curved beam is given by:

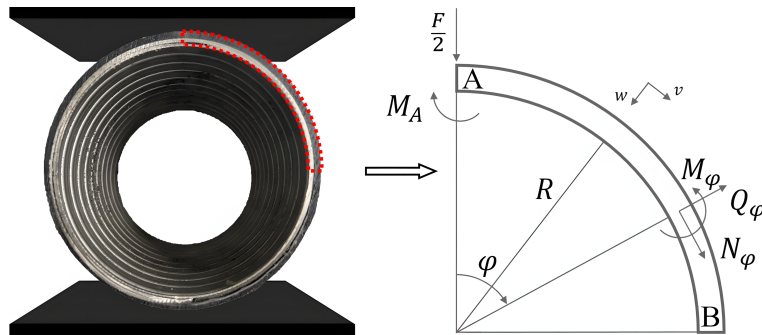


Figure 1: Mechanical model of flexible riser carcass under compression.

$$\frac{d^2w}{d\varphi^2} + w = -\frac{M_\varphi R^2}{EI} \quad (2)$$

The deflection equation of the flexible riser carcass subjected to flat-plate compression can hence be derived as:

$$\frac{d^2w}{d\varphi^2} + w = -\frac{M_A R^2}{EI} + \frac{FR^3}{2EI} \cdot \sin \varphi \quad (3)$$

The general solution to the above differential equation is the following:

$$w = -\frac{M_A R^2}{EI} - \frac{FR^3}{EI} \cdot \frac{\varphi \cos \varphi}{4} + C_1 \cos \varphi + C_2 \sin \varphi \quad (4)$$

As the rotation angle of the curved beam is given by $\theta = \frac{1}{R} \frac{dw}{d\varphi}$, taking the derivative of Equation (4) yields:

$$\theta = \frac{FR^2}{4EI} (\varphi \sin \varphi - \cos \varphi) - \frac{C_1}{R} \sin \varphi + \frac{C_2}{R} \cos \varphi \quad (5)$$

Similarly, according to the relation between the radial displacement w and the tangential displacement v (i.e., $w = \frac{dv}{d\varphi}$), the expression for the tangential displacement is:

$$v = -\frac{M_A R^2}{EI} \cdot \varphi - \frac{FR^3}{EI} \cdot \frac{\cos \varphi + \varphi \sin \varphi}{4} + C_1 \sin \varphi - C_2 \cos \varphi + C_3 \quad (6)$$

Boundary conditions based on symmetry can be established as $w(0) = w(\pi)$, $v(0) = v(\pi) = 0$. Additionally, the rotation angle at point A is zero, i.e., $\theta(0) = 0$. By substituting all these boundary conditions into Equation (4), we obtain:

$$[C_1 \ C_2 \ C_3 \ M_A] = \left[\frac{\pi FR^3}{8EI} \ \frac{FR^3}{4EI} \ \frac{FR^3}{2EI} \ \frac{FR}{\pi} \right] \quad (7)$$

Furthermore, the deflection curve of the curved beam in Figure 1 can be expressed as:

$$w = \frac{FR^3}{EI} \left(-\frac{1}{\pi} - \frac{\varphi \cos \varphi}{4} + \frac{\pi \cos \varphi}{8} + \frac{\sin \varphi}{4} \right) \quad (8)$$

The displacement obtained from the testing machine can be derived as:

$$X = 2 \cdot w(0) = \frac{\pi^2 - 8}{4\pi} \cdot \frac{FR^3}{EI} \quad (9)$$

In the current paper, the displacement is considered in an incremental form to incorporate the progressive development of material plasticity. Equation (9) in its incremental form is given by:

$$X_{\text{inc}} = 2 \cdot w(0) = \frac{\pi^2 - 8}{4\pi} \cdot \frac{F_{\text{inc}} R^3}{E_t I} \quad (10)$$

in which X_{inc} is the increment of the applied longitudinal displacement, F_{inc} is the increment of the measured reaction force from the testing machine, and E_t is the tangent modulus of the material.

Equation (10) can be further rewritten as:

$$\frac{F_{\text{inc}}}{X_{\text{inc}}} = \frac{\pi}{3(\pi^2 - 8)} \cdot \frac{Lt^3}{R^3} \cdot E_t \quad (11)$$

where L and t represent the length and the thickness of the flexible riser carcass layer, respectively.

Let $S_{\text{inc}} = \frac{F_{\text{inc}}}{X_{\text{inc}}}$, which is the local slope in Figure ??, we have:

$$E_t = S_{\text{inc}} \cdot \frac{3(\pi^2 - 8)}{\pi} \cdot \frac{R^3}{Lt^3} \quad (12)$$

On the other side, consider the stress at end A of the curved beam in Figure 1, which is the superposition of axial force-induced segment and bending moment-induced segment. Consequently, the following relationship can be derived:

$$\varepsilon = \frac{1}{E} (\sigma_N + \sigma_M) = \frac{6FR}{\pi E Lt^2} \quad (13)$$

Similarly, the expression of Equation (13) under an incremental step is:

$$\varepsilon_{\text{inc}} = \frac{6F_{\text{inc}}R}{\pi E_t Lt^2} \quad (14)$$

Substituting Equation (11) into Equation (14), we have:

$$\varepsilon_{\text{inc}} = \frac{2}{\pi^2 - 8} \cdot \frac{t}{R^2} \cdot X_{\text{inc}} \quad (15)$$

It can be observed that the left-hand sides of Equation (12) and Equation (15) correspond to the tangent modulus of the material and the associated strain increment under this modulus, respectively. In contrast, the right-hand sides are functions of X_{inc} , which can be derived from Figure 1. In deed, for any given X_{inc} , the tangent modulus E_t is the first derivative of the strain increment ε_{inc} , leading to the following differential equation:

$$F(E_t, \varepsilon_{\text{inc}}, X_{\text{inc}}) = 0 \quad (16)$$

By solving the above differential equation, a stress-strain curve can be obtained, which represents the equivalent material behaviour we aim to determine.

The critical buckling pressure of a classical ring is:

$$P_{\text{cri}} = \frac{3EI_{\text{eq}}}{R^3} \quad (17)$$

In the present paper, the tangent modulus method is employed to characterise the material plasticity evolution, with Equation 17 reformulated in the incremental form:

$$P_{\text{cri_inc}} = \frac{3E_t I_{\text{eq}}}{R^3} = \frac{t^3}{4R^3(1-\nu^2)} \cdot E_t \quad (18)$$

On the other hand, the prescribed radial displacement is applied to the ring incrementally. Based on the constitutive relation of the ring layer, the corresponding resisting pressure under each displacement increment can be further determined. Note that if the resisting external pressure obtained at a specific displacement increment equals the value calculated from Equation 18, this pressure is identified as the plastic collapse pressure of the ring layer. The result will be further compared to the numerical solutions in the subsequent sections.